

Isobaric Analog States and Coulomb Displacement Energies in the ($1d_{5/2}$) Shell*

J. C. HARDY, H. BRUNNADER, AND JOSEPH CERNY

Lawrence Radiation Laboratory and Department of Chemistry, University of California, Berkeley, California 94720

AND

J. JÄNECKE

Department of Physics, University of Michigan, Ann Arbor, Michigan 48104

(Received 31 January 1969)

The (p, t) and ($p, {}^3\text{He}$) reactions have been used to locate three previously unknown $T=\frac{3}{2}$ isobaric analog states in ${}^{19}\text{F}$, ${}^{19}\text{Ne}$, and ${}^{23}\text{Mg}$, in addition to significantly improving the precision on the energies of the $T=\frac{3}{2}$ state in ${}^{23}\text{Na}$ and the $T=2$ states in ${}^{20}\text{F}$ and ${}^{24}\text{Na}$. These multiplets all lie within the “($1d_{5/2}$) shell” in that they have fewer than $n=12$ nucleons outside ${}^{16}\text{O}$, and $T \leq \text{minimum}(\frac{1}{2}n, 6 - \frac{1}{2}n)$. Including these data, twenty-eight displacement energies are now known throughout this shell for all possible multiplets with $T \leq 2$ (except $T=2$, mass-22). The experimental displacement energies were compared in detail with calculations which used Hecht’s Coulomb-energy equations; the excellent agreement obtained appeared to be relatively insensitive to the assumed nuclear wave functions since both the low-seniority $j-j$ coupling limit and the Wigner supermultiplet scheme produced similar results. Four parameters related to the two-body Coulomb-energy matrix elements were treated as adjustable in fitting the data but their final values are in reasonable agreement with matrix elements calculated using harmonic-oscillator wave functions. A fifth adjustable parameter took account of the Z and N dependence of the charge radius. Using the experimental parameters, the unmeasured masses of ${}^{19}\text{Na}$, ${}^{20}\text{Mg}$, ${}^{21}\text{Mg}$, ${}^{22}\text{Al}$, ${}^{23}\text{Al}$, ${}^{24}\text{Si}$, and ${}^{25}\text{Si}$ are predicted, together with the excitation energies of unobserved analog states in the $1d_{5/2}$ shell.

I. INTRODUCTION

THE success of the isobaric multiplet mass equation in relating the masses of states within a multiplet has been remarkable.¹ It is now clear that if there are any deviations from its quadratic form they will probably be small, and their detection over a range of multiplets would require an experimental precision which is not yet possible. However, in first-order perturbation theory, *any* charge-dependent force of tensorial rank of two or less (two-body forces usually have these characteristics) will give rise to such a quadratic mass formula. Deviations from the quadratic form may be expected if a first-order perturbation treatment is not adequate. In order to examine the effects of non-Coulomb charge-dependent forces, the most valuable data would concern the variation of the coefficients in the quadratic mass formula as functions of mass number (A) and isospin (T). Since the Coulomb interaction is well understood, this (A, T) dependence can in principle be calculated under the assumption that the only charge-dependent forces are the Coulomb forces. One has to ascertain though that proper nuclear wave functions and charge radii are used and that higher-order perturbations are either small or properly taken into consideration. The latter may affect the quadratic term considerably.² Any experimental deviation from such detailed calculations may then be interpreted as being due to non-Coulomb forces such as charge-dependent nuclear forces or forces resulting from the electromagnetic spin-orbit interaction.

In order to minimize the number of extraneous effects,

* Work performed under the auspices of the U.S. Atomic Energy Commission.

¹ J. Cerny, *Ann. Rev. Nucl. Sci.* **18**, 27 (1968).

² J. Jänecke, *Bull. Am. Phys. Soc.* **13**, 1402 (1968).

it appeared desirable to carry out such an investigation within the confines of a single shell, and to discuss only the displacement energies (i.e., the energy differences between adjacent members of a multiplet), thus eliminating most of the effects of the nucleons in the core. We chose the $1d_{5/2}$ shell since, including the six measurements reported here, displacement energies are known within multiplets over the full range of possible A 's for all values of $T \leq 2$ with a single exception—the $T=2$ multiplet in mass 22. This makes the $1d_{5/2}$ shell more favorable than the $1f_{7/2}$ shell, which has been extensively investigated previously,³⁻⁶ because the former includes more measured displacement energies, they are known to greater precision, and completely cover the mass region⁷ for many values of T .

We report the location of three previously unobserved $T=\frac{3}{2}$ analog levels in ${}^{19}\text{F}$, ${}^{19}\text{Ne}$, and ${}^{23}\text{Mg}$, in addition to significantly improving the precision on the energy of the $T=\frac{3}{2}$ state in ${}^{23}\text{Na}$ and the $T=2$ states in ${}^{20}\text{F}$ and ${}^{24}\text{Na}$. These results are combined with all relevant experimental data previously obtained to produce 28 displacement energies throughout the shell.

In the past, some analyses of Coulomb-displacement energies^{5,6} have used the Coulomb-energy formula of Carlson and Talmi.⁸ This has met with surprising success

³ J. Jänecke, *Nucl. Phys.* **A114**, 433 (1968).

⁴ J. A. Nolen, J. P. Schiffer, N. Williams, and D. van Ehrenstein, *Phys. Rev. Letters* **18**, 1140 (1967).

⁵ M. Harchol, A. A. Jaffe, J. Mirion, I. Unna, and J. Zioni, *Nucl. Phys.* **A90**, 459 (1967).

⁶ R. Sherr, *Phys. Letters* **24B**, 321 (1967).

⁷ The notation “ $1d_{5/2}$ shell” is largely intended to reflect the fact that we consider states in nuclei with up to $n=12$ nucleons outside the ${}^{16}\text{O}$ core, but limited in isospin by $T \leq \text{minimum}(\frac{1}{2}n, 6 - \frac{1}{2}n)$.

⁸ B. C. Carson, and I. Talmi, *Phys. Rev.* **96**, 436 (1964); A. de-Shalit and I. Talmi, *Nuclear Shell Theory* (Academic Press Inc., New York, 1963).

considering that the formula was originally derived for proton configurations only and, as applied to n -nucleon systems of protons and neutrons, should only be valid if the seniority of the protons is a good quantum number. Recently, by considering the total isospin as a good quantum number, Hecht has derived Coulomb-energy formulas which apply specifically to a system of n neutrons and protons. These formulas have been derived in two limiting coupling schemes: the j - j coupling low-seniority scheme⁹ and the Wigner supermultiplet scheme.¹⁰ Since the Coulomb force is a long-range force, one might expect that the calculated displacement energies are relatively insensitive to the details of the assumed configurations. The theoretical formulas confirm these expectations by having a similar form in both the chosen coupling schemes. Thus, it is anticipated that the formulas should apply in intermediate coupling schemes as well. The theoretical equations are expressed in terms of matrix elements which we will parametrize, the five parameters being determined from a fit to the experimental data. The values so obtained will subsequently be compared with calculations which used harmonic-oscillator wave functions.

Such methods have already been applied with considerable success to the $1f_{7/2}$ shell,³ but only formulas for the seniority scheme were used. The present analysis of the $1d_{5/2}$ shell also provides the first examination of the importance of the coupling scheme assumed. We only examine displacement energies corresponding to the ground states of even- A nuclei and to the lowest $\frac{5}{2}^+$ states in odd- A nuclei. Even so, it is undoubtedly true that the wave functions of these states are not accurately represented by either coupling scheme considered. The fact that the formulas are quite successful in describing the experimental displacement energies is a reflection of the nature of the Coulomb force, and not of the accuracy of the assumed nuclear model. Nevertheless, the success of the formulas indicates that they can be used with confidence to predict masses of unmeasured neutron-deficient nuclei and excitation energies of unobserved analog states in the $1d_{5/2}$ shell. Such predictions will be tabulated.

II. EXPERIMENTAL PROCEDURE

All measurements reported here were made using the external 45-MeV proton beam from the Berkeley 88-in. spiral-ridge Cyclotron. After magnetic analysis, the beam had an energy resolution of 0.14% and was focused on a target at the center of the scattering chamber, a typical beam spot being 2 mm high by 1.5 mm wide. The exact angle at which the beam intersected the target was determined by observing via remote television two luminous foils, one at the target position and

the other 70 cm downstream. The beam current chosen for these experiments ranged from 60 to 800 nA, depending upon experimental conditions, and was monitored by a Faraday cup connected to an integrating electrometer. The energy of the beam was inferred from measuring its range in aluminum.

Reaction products were detected in two independent counter telescopes located on opposite sides of the scattering chamber. Each consisted of a 150- μ phosphorus-diffused silicon ΔE transmission counter operated in coincidence with a 3.0-mm lithium-drift silicon E counter; an additional 500- μ lithium-drift silicon E -reject counter was operated in anticoincidence with the first two, thus eliminating long-range protons and deuterons. A single 1-mm monitor counter was fixed at $\theta_{lab} = 27.5^\circ$ to observe any target deterioration or beam-energy changes during a series of measurements on a particular target.

For solid targets, a tantalum collimator 5 mm high by 2 mm wide was mounted 48 cm from the target, resulting in an angular resolution of 0.26° and an acceptance angle of 5×10^{-5} sr. Target gases were contained in a cell consisting of a cylindrical frame surrounded by a 315° continuous window of 2.5- μ Havar foil; the total enclosed volume was 47 cm³. In order to define the gas target and to eliminate particles scattered from the gas cell window, a second collimator with the same width as the first was mounted 36 cm ahead of it.

A schematic diagram of the electronics is shown in Fig. 1. The energy signals from the counters in each system, preamplified in the experimental area, were transmitted to the counting area where, after further amplification and satisfaction of slow coincidence ($2\tau \approx 2$ μ sec) requirements, they were fed to a Goulding-Landis particle identifier. An output signal characteristic of the particle type was produced, and by means of a four-channel router this signal was subsequently used to route the total-energy signal into 1024-channel groups of a 4096-channel analyzer. The spectra recorded for each telescope corresponded to α particles, ^3He particles, tritons, and those particles slightly less ionizing than the selected triton group. The first and last groups were taken primarily to check that no ^3He particle or triton counts were lost. The relative efficiencies of the two systems was checked in several runs where the telescopes were placed at the same angle but on opposite sides of the beam. The result obtained was 1.00 ± 0.05 .

The over-all energy resolution (full width at half-maximum) observed throughout was 100–130 keV for tritons and 120–150 keV for ^3He particles, depending upon the target used.

III. EXPERIMENTAL RESULTS

If a target nucleus has isospin T_i , then the ratio of the differential cross sections for (p, t) and $(p, ^3\text{He})$ reactions leading to analog final states with isospin $T_f = T_i + 1$ can be expressed simply when charge-

⁹ K. T. Hecht, Nucl. Phys. **A102**, 11 (1967).

¹⁰ K. T. Hecht, Nucl. Phys. **A114**, 280 (1968); see also K. T. Hecht and S. C. Pang (to be published).

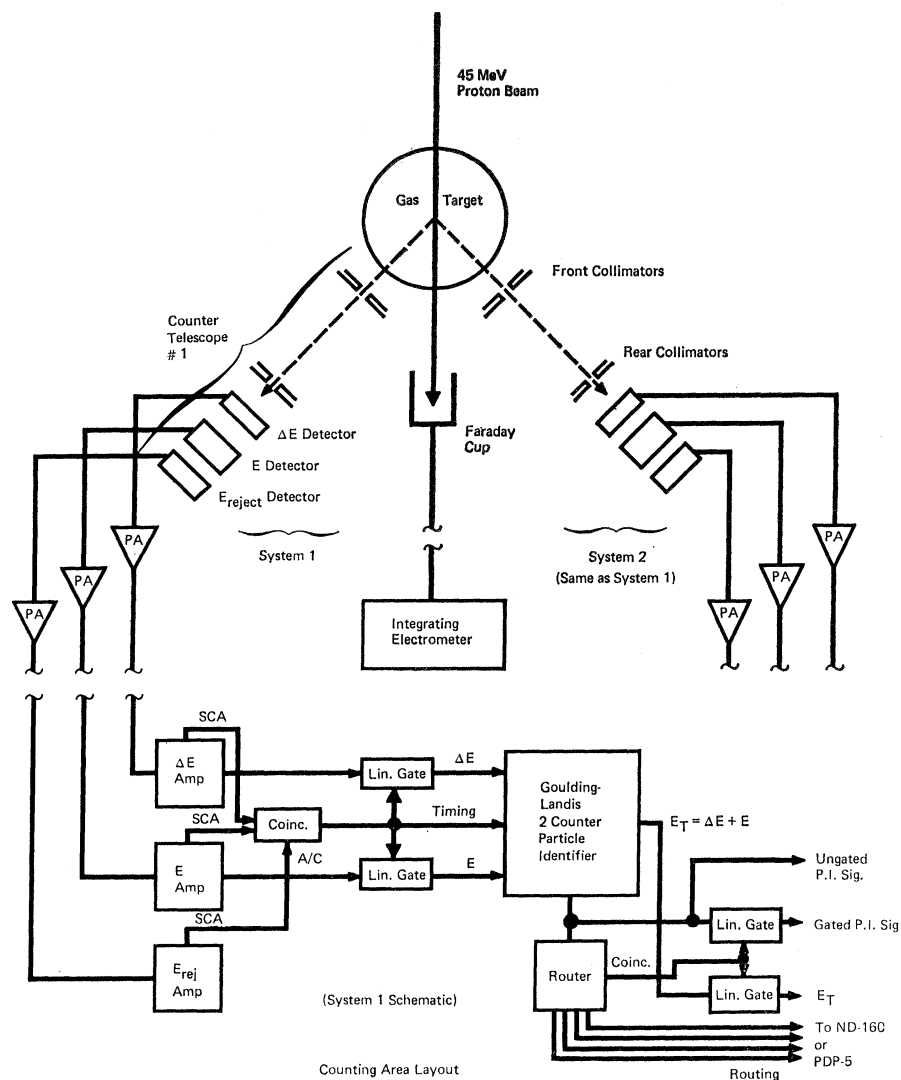


FIG. 1. Schematic diagram of the electronic setup used in conjunction with the two-counter particle identifier: Only system 1 is shown in its entirety, system 2 being identical.

dependent effects are neglected:

$$\frac{d\sigma/d\Omega(p, t)}{d\sigma/d\Omega(p, {}^3\text{He})} = \frac{k_t}{k_{3\text{He}}} \times \frac{2\langle (T_i+1)(T_{z_i}-1) 1 1 | T_i T_{z_i} \rangle^2}{\langle (T_i+1) T_{z_i} 1 0 | T_i T_{z_i} \rangle^2}. \quad (1)$$

Here k is the wave number of the outgoing particle and $\langle | \rangle$ is a Clebsch-Gordan coefficient. Thus, in this approximation, the differential cross sections to analog states should be identical in shape, and their magnitudes should be in the ratio $(k_t/k_{3\text{He}})$ when $T_f = \frac{3}{2}$ and $(2k_t/3k_{3\text{He}})$ when $T_f = 2$. These properties provide an unambiguous experimental method for identifying analog states.¹¹

The analog states having been identified, their excitation energies were determined by analyzing the

¹¹ J. Cerny and R. H. Pehl, Phys. Rev. Letters **12**, 619 (1964).

data with the computer program LORNA.¹² This program establishes an energy scale by finding a least-squares fit to peaks whose Q values are known, after correcting all incoming and outgoing particles for kinematic effects and absorber losses. For the data described here, contaminants were present or introduced in the targets, and well-known states produced from these contaminants were used in the calibrations. In particular, states produced from the reactions ${}^{12}\text{C}(p, t){}^{10}\text{C}$ and ${}^{12}\text{C}(p, {}^3\text{He}){}^{10}\text{B}$ were most useful throughout: The masses of the ground and first excited state of ${}^{10}\text{C}$ were taken from a recent reevaluation by Brunnader *et al.*¹³ while information on the levels of ${}^{10}\text{B}$ was taken from Ajzenberg-Selove and Lauritzen.¹⁴

¹² LORNA is a program written by C. C. Maples, whom we thank for making it available.

¹³ H. Brunnader, J. C. Hardy, and Joseph Cerny, Phys. Rev. **174**, 1247 (1968).

¹⁴ F. Ajzenberg-Selove and T. Lauritzen, Nucl. Phys. **A114**, 1 (1968).

TABLE I. Summary of experimental results.

Nucleus	Analog state J^π, T	This work (MeV \pm keV)	Excitation energy		Average value (MeV \pm keV)
			Previous work (MeV \pm keV)	Reference	
^{24}Mg	$0^+, 2$	15.426 ± 30	15.436 ± 5	15-17	15.436 ± 5
^{24}Na	$0^+, 2$	5.978 ± 35	5.98 ± 48	18, 19	5.979 ± 28
^{23}Mg	$\frac{5}{2}^+, \frac{3}{2}$	7.788 ± 25	not reported	...	7.788 ± 25
^{23}Na	$\frac{5}{2}^+, \frac{3}{2}$	7.910 ± 30	7.890 ± 30	21, 22	7.900 ± 21
^{20}Ne	$0^+, 2$	16.722 ± 25	16.732 ± 2.4	16, 23-25	16.732 ± 2.4
^{20}F	$0^+, 2$	6.523 ± 35	6.43 ± 100	23	6.513 ± 33
^{19}Ne	$\frac{3}{2}^+, \frac{3}{2}^a$	7.620 ± 25	not reported	...	7.620 ± 25
^{19}F	$\frac{3}{2}^+, \frac{3}{2}^a$	7.660 ± 35	not reported	...	7.660 ± 35

^a These levels are not the lowest-energy $T = \frac{3}{2}$ levels in mass 19, but are analogs to the first excited state (0.095 MeV) of ^{19}O .

A. $^{26}\text{Mg}(p, t)^{24}\text{Mg}$ and $^{26}\text{Mg}(p, {}^3\text{He})^{24}\text{Na}; T=2$ States

Figure 2 shows triton and ${}^3\text{He}$ spectra observed from a 1.26-mg/cm² self-supporting magnesium foil enriched to 99.2% in ^{26}Mg ; the data were taken at $\theta_{\text{lab}} = 22.3^\circ$ for 3200 μC . It is evident from the figure that a significant amount of carbon was present in the target, and the peaks corresponding to states in ^{10}C and ^{10}B provided the principal sources of calibration although all other peaks with (unbracketed) energies marked in the figure were also used.

The $T=2$ states in ^{24}Mg and ^{24}Na have both been identified previously¹⁵⁻¹⁹ and, in fact, the angular distribution of the (p, t) reaction to the state in ^{24}Mg has also been extensively studied.²⁰ Consequently, no attempt was made here to obtain angular distributions; both telescopes were set at $\theta_{\text{lab}} = 22.3^\circ$, this being near a maximum in the $L=0$ angular distribution as well as being an angle at which the analog states were resolved from nearby impurity levels. Values for the excitation energies were obtained and the results are given in Table I.^{15-19, 21-25} Also given in the table are weighted averages of all previous measurements, and a final overall average which also includes the present results.

Clearly, the precision of previous measurements¹⁵⁻¹⁷ of the $T=2$ state in ^{24}Mg precludes any improvement

¹⁵ G. T. Garvey, J. Cerny, and R. H. Pehl, Phys. Rev. Letters 12, 726 (1964).

¹⁶ E. Adelberger and A. B. McDonald, Phys. Letters 24B, 270 (1967); 24B, 618(E) (1967).

¹⁷ F. Riess, W. J. O'Connell, D. W. Heikkinen, H. M. Kuan, and S. S. Hanna, Phys. Rev. Letters 19, 327 (1967).

¹⁸ G. T. Garvey and J. Cerny (unpublished).

¹⁹ F. G. Kingston, R. J. Griffiths, A. R. Johnston, W. R. Gibson, and E. A. McClatchie, Phys. Letters 22, 458 (1966).

²⁰ S. W. Cospers, H. Brunnader, J. Cerny, and R. L. McGrath, Phys. Letters 25B, 324 (1967).

²¹ S. Mubarakmand and B. E. F. Macefield, Nucl. Phys. A98, 97 (1967); and (private communication).

²² J. Dubois, Nucl. Phys. A104, 657 (1967).

²³ J. Cerny, R. H. Pehl, and G. T. Garvey, Phys. Letters 12, 234 (1964).

²⁴ H. M. Kuan, D. W. Heikkinen, K. A. Snover, F. Riess, and S. S. Hanna, Phys. Letters 25B, 217 (1967).

²⁵ R. Bloch, R. E. Pixley, and P. Truöl, Phys. Letters 25B, 215 (1967).

by our value, but the excellent agreement between the two may be taken as a measure of the reliability of our methods.

B. $^{26}\text{Mg}(p, t)^{23}\text{Mg}$ and $^{26}\text{Mg}(p, {}^3\text{He})^{23}\text{Na}; T = \frac{3}{2}$ States

The spectra of tritons and ${}^3\text{He}$ observed from a 500- $\mu\text{g}/\text{cm}^2$ ^{26}Mg -enriched magnesium target are shown

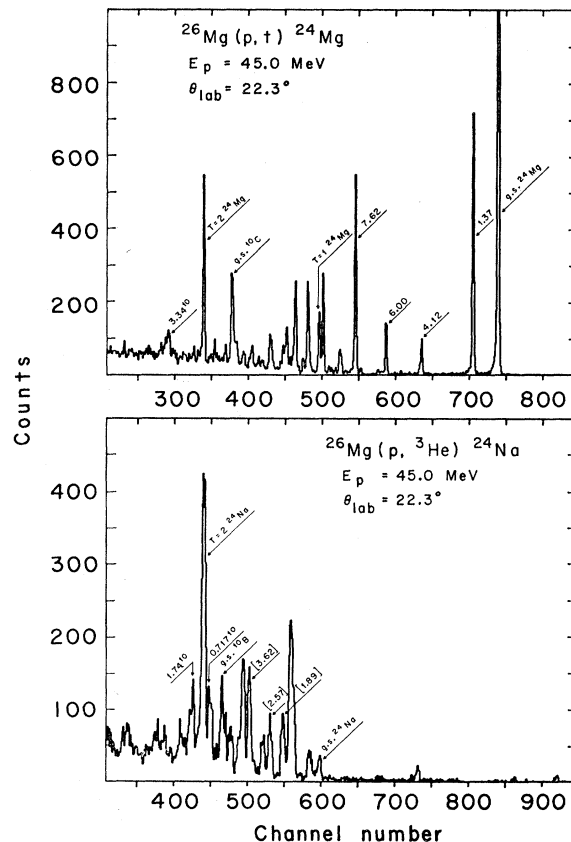


FIG. 2. Energy spectra of the reactions $^{26}\text{Mg}(p, t)^{24}\text{Mg}$ and $^{26}\text{Mg}(p, {}^3\text{He})^{24}\text{Na}$ taken at $\theta_{\text{lab}} = 22.3^\circ$ for 3200 μC . The target was 99.2% enriched in ^{26}Mg . All peaks whose energies are marked (unbracketed) were used to establish calibration; see text.

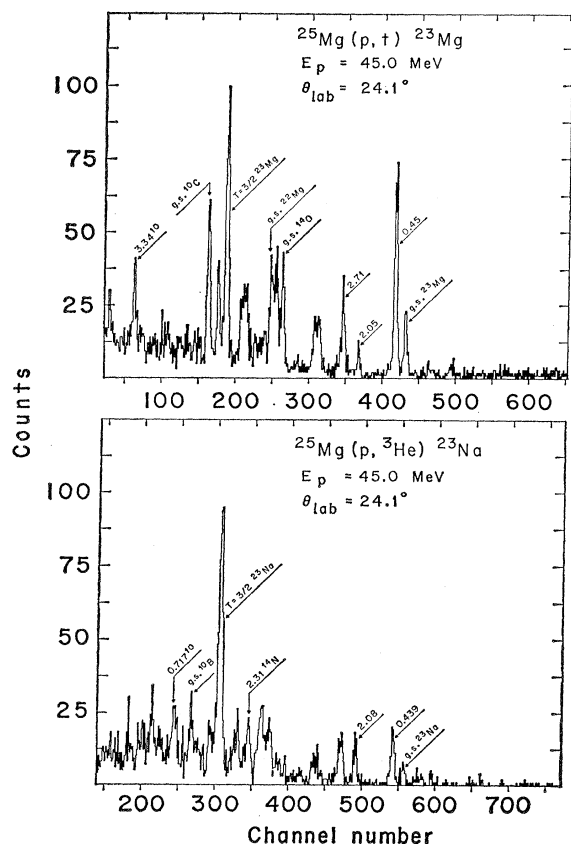


FIG. 3. Energy spectra of the reactions $^{25}\text{Mg}(p, t)^{23}\text{Mg}$ and $^{25}\text{Mg}(p, {}^3\text{He})^{23}\text{Na}$ taken at $\theta_{\text{lab}} = 24.1^\circ$ for $970 \mu\text{C}$. The target was 91.5% enriched in ^{25}Mg . All peaks whose energies are marked were used to establish calibration; see text.

in Fig. 3. The components of the target were ^{24}Mg (8.29%), ^{25}Mg (91.54%), ^{26}Mg (0.17%) and, in addition, oxygen and carbon impurities. Spectra were obtained at six angles between $\theta_{\text{lab}} = 17.2^\circ$ and 31.5° , with the data in the figure being collected for $970 \mu\text{C}$ at $\theta_{\text{lab}} = 24.1^\circ$.

Rough Coulomb-energy calculations indicate that the $T = \frac{3}{2}$ analog states should be at an excitation of about 7.8 MeV in ^{23}Mg and ^{23}Na . The peaks marked $T = \frac{3}{2}$ in Fig. 3 are consistent with these expectations, and at the top of Fig. 4 is shown the angular distribution of corresponding tritons and ${}^3\text{He}$ particles, the experimental

TABLE II. Optical-model parameters^a used in DWBA calculations.

Target	Projectile	V (MeV)	W_s (MeV)	r (fm)	a (fm)
$^{20}\text{Ne}, {}^{21}\text{Ne}$	p	51.5	19.0	1.25	0.5
	$t, {}^3\text{He}$	162.0	37.5	1.25	0.6
^{25}Mg	p	51.5	19.0	1.15	0.5
	$t, {}^3\text{He}$	162.0	37.5	1.15	0.6

^a Reference 20.

${}^3\text{He}$ points having been multiplied by $k_t/k_{{}^3\text{He}}$ ($=0.92$) in order to facilitate the comparison suggested by Eq. (1). The shapes and magnitudes of the distributions are the same within the expected accuracy of the approximations used in the derivation of Eq. (1) and thus, the $T = \frac{3}{2}$ character of the levels is established. Also shown at the bottom of Fig. 4 are the angular distributions for the (p, t) reaction to the ground state (gs) ($\frac{3}{2}^+$) and 0.451-MeV state ($\frac{5}{2}^+$) of ^{23}Mg . Since the spin parity of ^{25}Mg is $\frac{5}{2}^+$, the former transition should be characterized predominantly by $L=2$ transfer while the latter

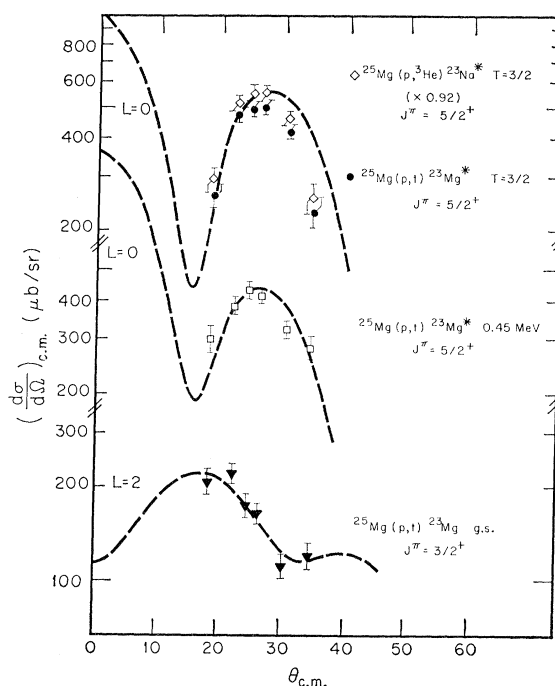


FIG. 4. Angular distributions of the reactions $^{25}\text{Mg}(p, t)^{23}\text{Mg}$ and $^{25}\text{Mg}(p, {}^3\text{He})^{23}\text{Na}$ leading to the $T = \frac{3}{2}$ analog states, the $(p, {}^3\text{He})$ cross section having been multiplied by 0.92 to correct for kinematic effects. The angular distributions of the (p, t) reaction leading to the $\frac{5}{2}^+$, 0.450-MeV state and to the $\frac{3}{2}^+$ ground state are also shown for comparison. The dashed curves are DWBA fits for the L values indicated, using the parameters given in Table II.

should have $L=0$. By a simple comparison, the angular momentum transfer to the analog states is determined to be predominantly $L=0$. To provide added confirmation, distorted-wave Born-approximation (DWBA) calculations were performed using a modified version of the computer program DWUCK^{26,27} and the optical-model potentials listed in Table II.²⁰ The results of computations which assumed pure $L=0$ or $L=2$ transfer are shown normalized to the experimental points in Fig. 4. Evidently, the spin parity of the $T = \frac{3}{2}$ states is $\frac{5}{2}^+$,

²⁶ The program DWUCK was written by D. Kuntz; we appreciate his making it available. The modification for two-nucleon transfer was made by us, and follows the "zero-range interaction" approximation (Ref. 27).

²⁷ N. K. Glendenning, Phys. Rev. **137**, B102 (1965).

indicating that they are analogs to the ground state of ^{23}Ne .

The energies of the analog states were determined precisely by using, as known, the peaks whose energies are marked in Fig. 3; the principal calibration points in the (p, t) spectrum were the gs of ^{10}C , ^{22}Mg , and ^{14}O while in the $(p, ^3\text{He})$ spectrum they were the gs of ^{10}B and the 2.31-MeV state ($T=1$) in ^{14}N . The results are given in Table I where, for the case of the $T=\frac{3}{2}$ level in ^{23}Na , it can be seen that there is good agreement with earlier measurements.^{21,22} There has been no previous observation reported of the analog state in ^{23}Mg .

C. $^{22}\text{Ne}(p, t)^{20}\text{Ne}$ and $^{22}\text{Ne}(p, ^3\text{He})^{20}\text{F}$; $T=2$ States

In order to provide internal calibration points in the region of the $T=2$ analog states in mass 20, a mixture of 50% neon and 50% methane was used. The neon gas was 92.0% enriched in ^{22}Ne , the proportions of the remaining isotopes being 7.6% ^{20}Ne and 0.4% ^{21}Ne .

As was the case with the $T=2$ states in mass 24, the lowest analog states in ^{20}Ne and ^{20}F have been identified previously,^{16,23-25} so no angular distributions were obtained in this experiment. Figure 5 shows triton and

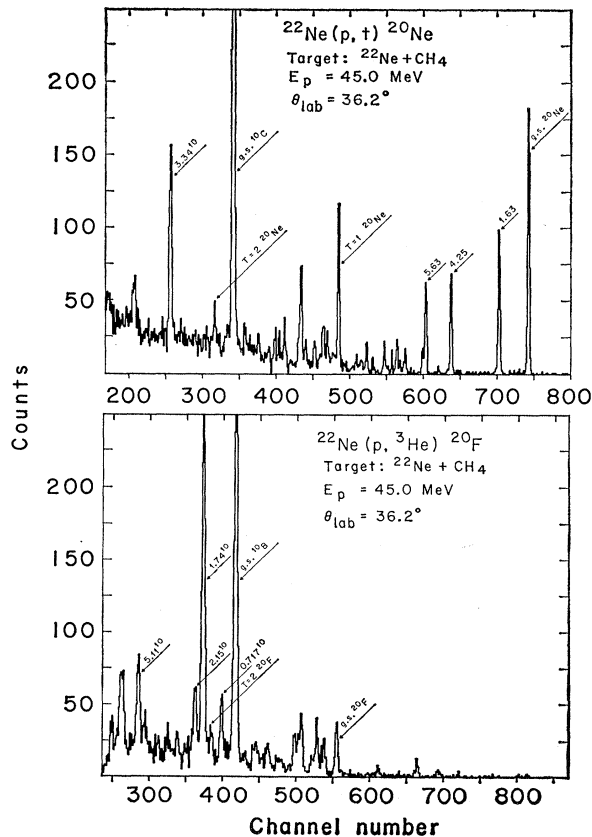


FIG. 5. Energy spectra of the reactions $^{22}\text{Ne}(p, t)^{20}\text{Ne}$ and $^{22}\text{Ne}(p, ^3\text{He})^{20}\text{F}$ taken at $\theta_{\text{lab}}=36.2^\circ$ for 9280 μC . The target was a 50:50 mixture of neon and methane, the neon being 92.0% enriched in ^{22}Ne . All peaks whose energies are marked were used to establish calibrations; see text.

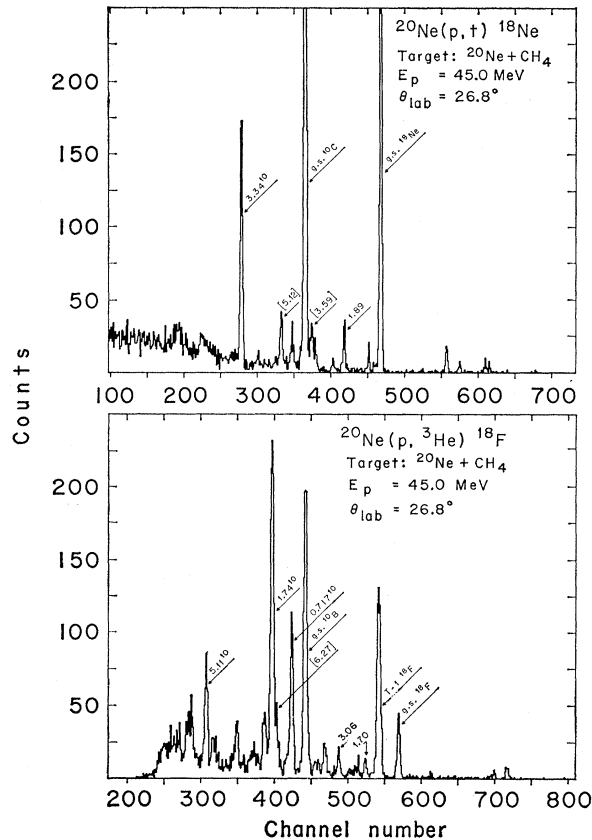


FIG. 6. Energy spectra of the reactions $^{20}\text{Ne}(p, t)^{18}\text{Ne}$ and $^{20}\text{Ne}(p, ^3\text{He})^{18}\text{F}$ taken at $\theta_{\text{lab}}=26.8^\circ$ for 2570 μC . The target was a 40:60 mixture of neon and methane, the neon being 99.9% enriched in ^{20}Ne . All peaks whose energies are marked (unbracketed) were used to establish calibrations; see text.

^3He spectra taken at $\theta_{\text{lab}}=36.2^\circ$ for 9280 μC . Although the cross section for $L=0$ transfer is relatively low at this angle, it is greater than for any other angle at which both $T=2$ states are simultaneously resolved. The energies of the analog states were again determined principally using states in ^{10}C and ^{10}B for calibration. The result for ^{20}Ne appears directly in Table I and agrees well with previous measurements. Additional data pertaining to the analog state in ^{20}F was provided by the experiment described in Sec. III (E), and it is the average of all data on this state which appears in Table I.

D. $^{20}\text{Ne}(p, t)^{18}\text{Ne}$ and $^{20}\text{Ne}(p, ^3\text{He})^{18}\text{F}$; $T=1$ States

In order to calibrate the $^{21}\text{Ne}(p, t)^{19}\text{Ne}$ and $^{21}\text{Ne}(p, ^3\text{He})^{19}\text{F}$ spectra which will be presented in the next section, it was necessary to establish the excitation energy of the states produced from the ^{20}Ne present in that target. For this purpose, a mixed neon (40%) and methane (60%) target was used, the neon being 99.9% enriched in ^{20}Ne . Spectra were taken at four angles between $\theta_{\text{lab}}=22.3^\circ$ and 41.0° ; spectra collected for 2570 μC at $\theta_{\text{lab}}=26.8^\circ$ are shown in Fig. 6. The states

TABLE III. Excited states of ^{18}Ne .

This work (MeV \pm keV)	Previous work (MeV \pm keV)	Average (MeV \pm keV)
g.s.	g.s.	—
1.890 \pm 20	1.8873 \pm 0.2 ²⁸	1.8873 \pm 0.2 ^a
3.375 \pm 30	3.3762 \pm 0.4 ²⁸	3.3762 \pm 0.4
3.588 \pm 25 ^{a,b}	{ 3.5763 \pm 2.0 ²⁸ 3.6164 \pm 0.6 ²⁸	{ 3.5763 \pm 2.0 3.6164 \pm 0.6
4.580 \pm 30	4.558 \pm 13.5 ^{29,30}	4.562 \pm 12.2
5.115 \pm 25	5.140 \pm 18 ²⁹	5.132 \pm 15 ^a

^a These values were used as known in the analysis of $^{21}\text{Ne}(p, t)^{19}\text{Ne}$.

^b This value was used in the analysis of $^{21}\text{Ne}(p, t)^{19}\text{Ne}$ because it represents the effective energy of the unresolved mixture of the (0^+) state at 3.5763 MeV, and the $2^{(+)}$ state at 3.6164 MeV, both populated by the (p, t) reaction.

whose energies are marked without brackets in the figure were used to establish the mass-18 calibration, and the excitation energies thus determined for states observed in ^{18}Ne are listed in Table III together with previous measurements²⁸⁻³⁰ and final averages. Those values which are noted in the table will be used in the following section.

Since the density of states above ~ 4 MeV in ^{18}F is large, it is difficult to make a meaningful comparison of states observed by us with those observed previously. However, there is only one state which is necessary for subsequent calibration and the excitation energy we obtain is 6.27 ± 0.03 MeV³¹; this should be compared with 6.265 ± 0.013 MeV measured³² in the reaction $^{16}\text{O}(^3\text{He}, p)^{18}\text{F}$, and it is the latter value which will be used.

E. $^{21}\text{Ne}(p, t)^{19}\text{Ne}$ and $^{21}\text{Ne}(p, ^3\text{He})^{19}\text{F}$; $T = \frac{3}{2}$ States

The neon target used was enriched in ^{21}Ne , with an isotopic composition of 21.1% ^{20}Ne , 56.3% ^{21}Ne and 22.6% ^{22}Ne . A range of seven angles from $\theta_{\text{lab}} = 11.7^\circ$ to 31.5° was studied in order to obtain angular distributions. Spectra collected for 4880 μC at $\theta_{\text{lab}} = 22.3^\circ$ are shown in Fig. 7.

Rough Coulomb-energy calculations predict the $T = \frac{3}{2}$ analog levels in ^{19}Ne and ^{19}F to be at about 7.5 MeV. The peaks marked $T = \frac{3}{2}^*$ in Fig. 7 are consistent with that value, and the angular distribution of corresponding triton and ^3He particles is shown at the top of Fig. 8, where the ^3He points have been multiplied by $k_t/k_{^3\text{He}}$ ($=0.93$). The similarity of the distributions

²⁸ R. D. Gill, B. C. Robertson, J. L'Ecuyer, R. A. I. Bell, and H. J. Rose, Phys. Letters **28B**, 116 (1968).

²⁹ E. Adelberger, thesis, California Institute of Technology (unpublished).

³⁰ J. H. Towle and G. J. Wall, Nucl. Phys. **A118**, 500 (1968).

³¹ Although this peak is not clearly resolved in Fig. 6 from the 1.74-MeV state in ^{19}B , it should be pointed out that this was not the case at the other angles observed.

³² Nolan F. Mangelson, B. G. Harvey, and N. K. Glendenning, Nucl. Phys. **A117**, 161 (1968).

satisfies the requirements of Eq. (1) and identifies the levels as being $T = \frac{3}{2}$. Triton angular distributions characteristic of $L=0$ and $L=2$ transfer are also shown for two $T = \frac{1}{2}$ levels in ^{19}Ne ; in addition the $L=0$ distribution is included for the (p, t) reaction on ^{20}Ne leading to the ground state of ^{18}Ne . DWBA fits are also shown in which the computations used the optical-model parameters listed in Table II. Clearly, the analog states are produced by an $L=0$ transfer, and since the ground state of ^{21}Ne is $\frac{3}{2}^+$, these states³³ must also have $J^\pi = \frac{3}{2}^+$. However, the spin parity of the ^{19}O ground state is $\frac{5}{2}^+$, indicating that the $T = \frac{3}{2}$ states we produce in ^{19}Ne and ^{19}F must presumably be analogs to the first excited state of ^{19}O —a $\frac{3}{2}^+$ state at 0.095 MeV.

The excitation energies of the analog states were determined in the manner previously described, the results being listed in Table I. There have been no previously reported measurements of either value although

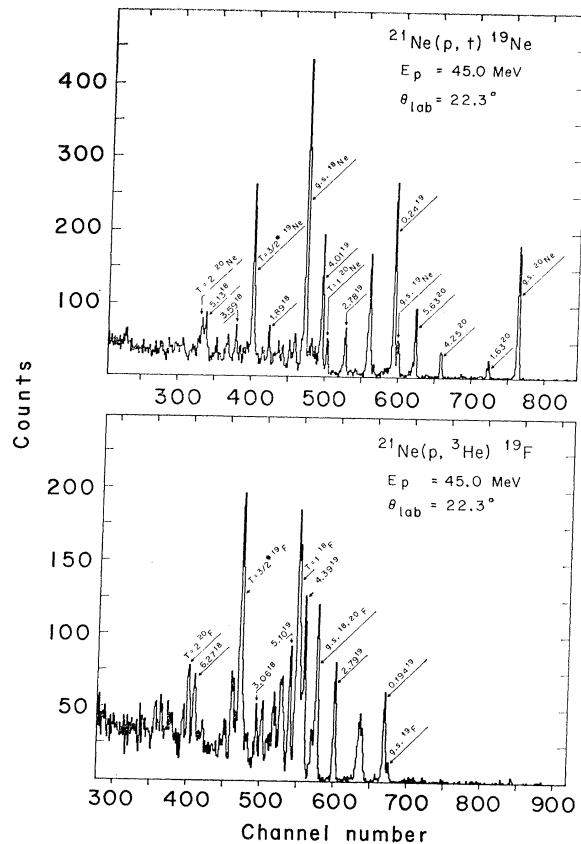


FIG. 7. Energy spectra of the reactions $^{21}\text{Ne}(p, t)^{19}\text{Ne}$ and $^{21}\text{Ne}(p, ^3\text{He})^{19}\text{F}$ taken at $\theta_{\text{lab}} = 22.3^\circ$ for 4880 μC . The neon target was enriched to 56.3% in ^{21}Ne , and included 21.1% ^{20}Ne and 22.6% ^{22}Ne . All peaks whose energies are marked were used to establish calibrations; see text.

³³ There are no states in ^{19}Ne known to be $\frac{3}{2}^+$ and consequently there could be no "known" $L=0$ angular distributions to states in that nucleus. Instead, for comparison, the $L=0$ distribution of the $^{20}\text{Ne}(p, t)^{18}\text{Ne}$ g.s. was used in Fig. 8. It should be noted however, that the obvious $L=0$ distribution to the 4.013-MeV state in ^{19}Ne identifies it, as well as the analog state, to be $\frac{3}{2}^+$.

an observation has been reported³⁴ of the lowest $T = \frac{3}{2}$ state in ^{19}F .

The calibration of the ^3He spectrum also yielded an energy for the $T = 2$ state in ^{20}F , the accuracy of which depends in large part upon the 6.265 ± 0.013 MeV state in ^{18}F . As mentioned earlier, the value quoted in Table I for the analog state in ^{20}F is an average of this value and the one obtained in Sec. III C.

IV. COULOMB DISPLACEMENT ENERGIES—CALCULATIONS

The potential which describes the Coulomb interaction between nucleons can be written as the sum of three operators, respectively having the properties of a scalar, a vector, and a tensor in isospin space.^{10,35} A general expression for the Coulomb energy of a nuclear state which involves A nucleons can be derived from this interaction using first-order perturbation theory. The result for a state with total isospin T and $T_z = \frac{1}{2}(N - Z)$ is

$$E_c(A, T, T_z) = E^{(0)}(A, T) - T_z E^{(1)}(A, T) + [3T_z^2 - T(T+1)]E^{(2)}(A, T). \quad (2)$$

The isoscalar, isovector, and isotensor coefficients $E^{(0)}$, $E^{(1)}$, and $E^{(2)}$ depend only upon A , T , and the details of the space-spin structure of the nuclear wave functions. They can be directly related to the coefficients in the isobaric multiplet mass equation (IMME)³⁶:

$$M(A, T, T_z) = a(A, T) + b(A, T)T_z + c(A, T)T_z^2. \quad (3)$$

The IMME has been used successfully to describe the energies of states within isobaric multiplets with $T > 1$ and with the possible exception of mass 9. No deviations from its predictions have been detected experimentally.¹ This result implies that for the cases under consideration a second- or higher-order perturbation treatment of the Coulomb interaction is not necessary, or alternately that the effect of such a treatment is mostly absorbed by the coefficients of the quadratic equation.² In addition to the Coulomb interaction, other small charge-dependent effects such as the charge-dependent nuclear interaction and the electromagnetic spin-orbit interaction can also be treated as simple perturbations without affecting the form of the quadratic IMME. This means that an experimental determination of the coefficients in the IMME will include not only the effects of the Coulomb interaction but also other small charge-dependent effects. Ultimately, a compari-

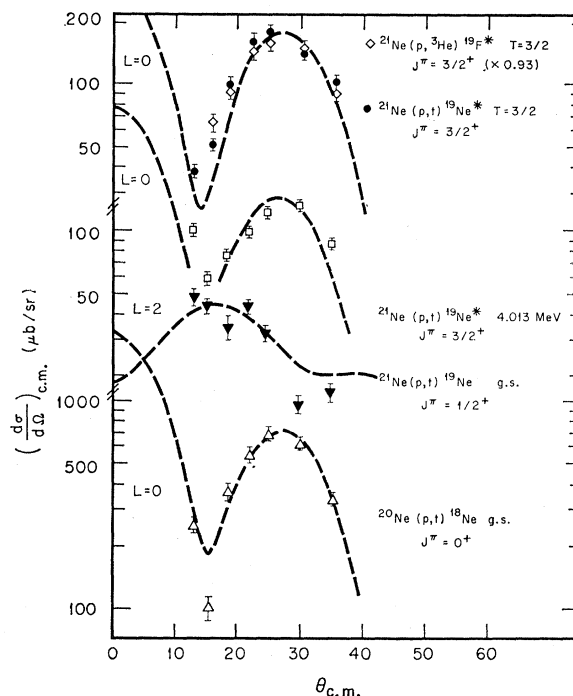


FIG. 8. Angular distributions of the reactions $^{21}\text{Ne}(p, t)^{19}\text{Ne}$ and $^{21}\text{Ne}(p, ^3\text{He})^{19}\text{F}$ leading to the $T = \frac{3}{2}$ analog states, the $(p, ^3\text{He})$ cross section having been multiplied by 0.93 to correct for kinematic effects. The angular distributions of the reaction $^{21}\text{Ne}(p, t)^{19}\text{Ne}$, leading to the 4.013-MeV and ground states, as well as that of the reaction $^{20}\text{Ne}(p, t)^{18}\text{Ne}$ leading to the ground state, are shown for comparison. The dashed curves are DWBA fits for the L values indicated, using the parameters given in Table II.

son with calculations which include only Coulomb effects should yield a magnitude for any additional charge dependence. Such calculations, however, must be based on realistic nuclear wave functions using proper radii and they must, if necessary, include the corrections from a higher-order perturbation treatment.

The purpose of the present investigation is to compare the experimental and calculated Coulomb displacement energies in the $1d_{5/2}$ shell. In terms of those quantities defined in Eq. (2) the Coulomb displacement energy between neighboring isobars is given by

$$\Delta E_c(A, T, T_z - 1 | T_z) \equiv E_c(A, T, T_z - 1) - E_c(A, T, T_z) = E^{(1)}(A, T) - 3(2T_z - 1)E^{(2)}(A, T). \quad (4a)$$

The corresponding experimental quantity is

$$M(A, T, T_z - 1) - M(A, T, T_z) + \Delta m, \quad (4b)$$

where Δm is the neutron-hydrogen mass difference ($= 0.7824$ MeV). Any discrepancy between calculations using Eq. (4a) and the experimental quantities (4b) may be interpreted as arising from one or several of the following factors: (i) the approximate nature of the nuclear wave functions used in the calculations; (ii) mathematical approximations introduced into the calculations, for example, by neglecting small terms;

³⁴ J. W. Butler, L. W. Fagg, and H. D. Holmgren, Phys. Rev. **113**, 268 (1959).

³⁵ J. Jänecke, Phys. Rev. **147**, 735 (1966).

³⁶ E. P. Wigner, in *Proceedings of the Robert A. Welch Foundation Conference on Chemical Research*, edited by W. O. Milligan (The Robert A. Welch Foundation, Houston, Texas, 1958), p. 67; S. Weinberg and S. B. Treiman, Phys. Rev. **116**, 465 (1959); D. H. Wilkinson, in *Isobaric Spin in Nuclear Physics*, edited by J. D. Fox and D. Robson (Academic Press Inc., New York, 1966), p. 30.

TABLE IV. Coefficients in the expansion of the Coulomb displacement energy, $\Delta E_c(A, T, T_z-1 | T_z) = [a + (n-2T_z)b + A_1c^{(1)} + A_2c^{(2)}] [f(\lambda)]^{-1}$, where A_1 and A_2 are listed for configurations j^n in the seniority scheme.

v	t	J	A_1	A_2
0	0	0	0	$-(2T_z-1) \left[1 + \frac{(2j+4)^2 - (n-2j-1)^2}{(2T-1)(2T+3)} \right]$
1	$\frac{1}{2}$	j	$\frac{(n-2j-1) - (-)^{n/2-T}(2T+1)(2j+3)}{2T(T+1)}$	$-(2T_z-1) \left[1 + \frac{(2j+3)^2 - (n-2j-1)^2}{4T(T+1)} \right]$
2	0	odd	0	$-(2T_z-1) \left[1 + \frac{(2j+2)^2 - (n-2j-1)^2}{(2T-1)(2T+3)} \right]$
2	1	even, >0	$\frac{2(n-2j-1)}{T(T+1)}$	$-(2T_z-1) \left[1 + \frac{(2j+1)(2j+3) - (n-2j-1)^2}{T(T+1)} - \frac{3(2j+2)^2 - 3(n-2j-1)^2}{(2T-1)(2T+3)} \right]$

(iii) the presence of isospin mixing, which means that the $(2T+1)$ members of a multiplet are not simply related by the isospin ladder operators T_{\pm} , and indicates that the first-order perturbation treatment used to derive Eq. (2) is no longer sufficient; and (iv) the presence of charge-dependent forces other than Coulomb forces.

Our approach will entail parametrizing Eq. (4a) according to calculations based on simple shell-model states and two different coupling schemes. The parameters will then be determined from a fit to data throughout the $1d_{5/2}$ shell, and only the final parameter values will be used for comparison.

A. Low-Seniority Limit of the j - j Coupling Scheme

Theoretical expressions for $E^{(1)}$ and $E^{(2)}$ have been derived by Hecht⁹ for shell-model states having the configuration j^n and seniority $v < 2$, the representation being chosen such that each state is defined by the four quantum numbers v , t (reduced isospin), J , and T . These expressions are given in terms of two-body Coulomb-energy matrix elements

$$V_{J'} = \langle j^2 J' | e^2/r_{ij} | j^2 J' \rangle, \quad (5)$$

and the interaction of the protons in the j shell with those in the core

$$a_c = \sum_{J', J_c} \frac{(2J'+1)}{(2j+1)} \langle (jj_c) J' | e^2/r_{ij} | (jj_c) J' \rangle. \quad (6)$$

In his formulation, the three quantities which must be evaluated or treated as free parameters are a_c , b and c , where

$$b = \frac{2(j+1)\bar{V}_2 - V_0}{2(2j+1)}, \quad c = \frac{V_0 - \bar{V}_2}{4(2j+1)}. \quad (7)$$

Here \bar{V}_2 is the average seniority-2 matrix element.

Expressions for $E^{(1)}$ and $E^{(2)}$ may now be obtained³⁷ in terms of these quantities with the use of Table 1 of Ref. 10. As detailed below, we have generalized Hecht's expressions in the manner described by Jänecke³ so as to take account of additional non-Coulomb charge-dependent effects and the variation of the nuclear radius with mass number. This results in an increase in the number of free parameters to five.

The additional charge dependence will be expected to have the greatest effect upon the quantity c . In particular, the electromagnetic spin-orbit interaction³⁸ between nucleons is expected to cause an increase in this parameter of as much as 40%. Furthermore, its increase in the tensor coefficient should be greater than in the vector coefficient by a factor ~ 1.7 [$= (g_p - g_n)/g_p$]. Consequently, we replace the quantity c by $c^{(1)}$ in the vector coefficient and by $c^{(2)}$ in the tensor coefficient. It is important to note that $c^{(1)}$ and $c^{(2)}$ will in addition contain the effects of charge dependence in the nuclear force, but since these quantities are relatively small, any inadequacy in the assumed wave functions or any approximation introduced into the calculation might also be expected to affect the values of $c^{(1)}$ and $c^{(2)}$ determined from experimental data.

The variation of the charge radius with mass number affects the values of the matrix elements in Eqs. (5) and (6). The Coulomb interaction radius R which is defined for any pair of protons will be assumed to vary according to

$$R \equiv \langle (j_1 j_2) J' | r_{ij}^{-1} | (j_1 j_2) J' \rangle^{-1} = R_0 [1 + \frac{1}{3} \lambda (n/N)] \\ \equiv R_0 f(\lambda), \quad (8)$$

³⁷ The expressions in Ref. 10 may be shown equivalent to those appearing in Eqs. (86)–(90) of Ref. 9, by utilizing the relation

$$V_{\text{even}} = \bar{V}_0/j(2j+1) + \bar{V}_2(2j-1)(j+1)/j(2j+1).$$

Note in addition that our definitions of the various matrix elements differ by a factor of 3 from those in Refs. 9 and 10.

³⁸ K. T. Hecht, *Isobaric Spin in Nuclear Physics*, edited by J. D. Fox and D. Robson (Academic Press Inc., New York, 1966), p. 823.

TABLE V. Coefficients in the expansion of the Coulomb displacement energy, $\Delta E_c(A, T, T_z-1 | T_z) = [a' + (n-2T_z)b' + A_1c^{(1)} + A_2c^{(2)}] [f(\lambda)]^{-1}$, where A_1 and A_2 are listed for various ground-state configurations in the d shell using the supermultiplet scheme. The Wigner supermultiplet quantum numbers are denoted by $[\tilde{f}]$.

$[\tilde{f}]$	S	J	$\frac{1}{2}n-T$	x	A_1	A_2
$[x+y, x+y, x, x]^a$	0	0	even	$\frac{1}{4}(n-2T)$	0	$-(2T_z-1)[6/(2T-1)]$
$[x+y, x+y, x+1, x]$	$\frac{1}{2}$	$\frac{3}{2}, \frac{5}{2}$	odd	$\frac{1}{4}(n-2T-2)$	$-(-)^{n/2-T}[3/T]$	$-(2T_z-1)[3/T]$
$[x+y, x+y-1, x, x]$	$\frac{1}{2}$	$\frac{3}{2}, \frac{5}{2}$	even	$\frac{1}{4}(n-2T)$		
$[x+2, x+1, x+1, x]^b$	0, 1	2, 3, 4	odd	$\frac{1}{4}(n-4)$	0	$(2T_z-1)[6-4S(S+1)]$

^a $T > 0$.

^b Only applies to ground states when $T = 1$.

where n is the number of active nucleons, N is the number of nucleons in the core, and R_0 is a constant. The quantities R and R_0 depend upon the values of j, j_c (if a core proton is involved) and J' ; the function $f(\lambda)$ is assumed to be the same for all proton pairs. Equation (8) may be considered as the first term of a binomial expansion and, for $\lambda=1$, would correspond approximately to an $A^{1/3}$ dependence of R . In the $1d_{5/2}$ shell Eq. (10) becomes

$$R = R_0[1 + \frac{1}{3}\lambda(A-16)/16],$$

treating λ as a free parameter.

Having made these modifications, one may use Eq. (4a) to obtain a final expression for the Coulomb displacement energy which has the form

$$\Delta E_c(A, T, T_z-1 | T_z) = [a + b(n-2T_z) + A_1c^{(1)} + A_2c^{(2)}] [f(\lambda)]^{-1}, \quad (9)$$

where $a = a_c + 4(j+1)c^{(1)}$. In Table IV we have quoted general formulas³⁹ for the coefficients A_1 and A_2 , assuming j^n configurations with $v \leq 2$; they were all calculated using the expressions for $E^{(1)}$ and $E^{(2)}$ given in Table 1 of Ref. 10. The expressions for the $v=2$ cases had already been simplified by making use of the fact that, to a good approximation,³ $V_{J'} = \bar{V}_2$ for all J' (even) ≥ 2 .

B. Wigner Supermultiplet Scheme

Hecht¹⁰ has derived general algebraic formulas for $E^{(1)}$ and $E^{(2)}$ assuming certain configurations in the Wigner supermultiplet scheme.⁴⁰ The supermultiplet quantum numbers, the total spin S , and the isospin T were assumed to be good quantum numbers. Thus, the states are identified by L, S, T , and $[\tilde{f}]$, where $[\tilde{f}]$ is the partition which characterizes a particular irreducible representation^{41,42} of U_4 . The form of $[\tilde{f}]$ is given by

$$[\tilde{f}] \equiv [x_1, x_2, x_3, x_4],$$

³⁹ It should be noted that the formulas for $v=0$ and $v=1$ are simply generalizations of Eqs. (6) and (7) of Ref. 3, where they were written exclusively for the $\frac{3}{2}$ shell.

⁴⁰ E. Wigner, Phys. Rev. **51**, 106 (1937).

⁴¹ H. A. Jahn, Proc. Roy. Soc. (London) **A201**, 516 (1950).

⁴² H. A. Jahn and H. van Wieringen, Proc. Roy. Soc. (London) **A209**, 502 (1951).

where

$$\sum_{i=1}^4 x_i = n$$

is the number of nucleons in the major oscillator shell, and $x_i \geq x_k$ when $i < k$. The Coulomb energies were assumed to be independent of the spatial quantum numbers. This should be a good approximation, but the expressions are even exact if applied to the average Coulomb energies for all states of an SU_6 multiplet in the $1d\ 2s$ shell.

The supermultiplet quantum numbers of the ground states have been predicted by Jahn⁴¹ for nuclei throughout the d shell. From these predictions certain patterns are apparent, and by using the formulas in Ref. 10 we have derived general expressions for Coulomb displacement energies which apply to most ground-state supermultiplets throughout the shell. The result is the same as Eq. (9) except that $a = a_c + 6c^{(1)}$ and the formulas for A_1 and A_2 are different. The coefficients a_c, b , and $c^{(i)}$ can be expressed in terms of the two-body Coulomb-energy matrix elements which are the orbital angular momentum analogs of the corresponding matrix elements in the seniority scheme.

General formulas for A_1 and A_2 with various ground-state configurations are shown in Table V. The only cases for which the existing formulas are insufficient are those multiplets based on the ground states of odd-odd nuclei with $T > 1$. A comparison of the formulas listed in Table V with those listed in Table IV shows a number of striking similarities in spite of the dissimilarity of the coupling schemes used in their calculation. Although both extreme coupling schemes are probably inadequate to describe nuclear states in this mass region, these similarities do suggest that the formulas for displacement energies might nevertheless accurately reproduce and predict experimental data. This is not an unexpected conclusion since the long range of the Coulomb force precludes any strong dependence upon the configuration assignment.

V. COULOMB DISPLACEMENT ENERGIES—COMPARISON WITH EXPERIMENT

A complete summary of experimentally determined Coulomb displacement energies throughout the $1d_{5/2}$

TABLE VI. Experimental and calculated Coulomb displacement energies.

A	T	T _z	J ^π	Experimental ΔE _c (A, T, T _z -1 T _z) (keV)	Seniority calculations		Supermultiplet calculations	
					ΔE _c (keV)	ΔE _c (calc) -ΔE _c (expt) (keV)	ΔE _c (keV)	ΔE _c (calc) -ΔE _c (expt) (keV)
17	½	+½	½+	3542.0±1.0 ^a	3542.2	0.2	3542.8	0.6
19	½	+½	½+ ^b	4060.8±2.0 ^{e,d}	4104.3	43.5 ^e	4103.2	42.4 ^e
21	½	+½	½+ ^b	4315.3±8.3 ^{e,f}	4316.6	1.3	4314.8	-0.5
23	½	+½	½+ ^r	4850.5±4.7 ^e	4861.1	10.6	4860.0	9.5
25	½	+½	½+	5062.5±1.1 ^e	5062.6	0.1	5062.2	-0.3
27	½	+½	½+	5592.5±3.2 ^e	5590.3	-2.2	5592.8	0.3
18	1	+1	0+	3478.9±1.0 ^{a,h}	3549.4	70.5 ^e	3510.4	31.5 ^e
20	1	+1	2+	4027.8±8.4 ^{e,i}	4024.9	-2.9
22	1	+1	0+	4282.1±2.2 ^{e,j}	4279.0	-3.1	4280.0	-2.1
24	1	+1	4+	4783.5±4.6 ^{e,k}	4790.2	6.7
26	1	+1	0+	5014.8±4.2 ^e	5021.1	6.3	5025.0	10.2
18	1	0	0+	4187.6±3.8 ^{a,b}	4142.8	-44.8 ^e	4137.6	-50.0 ^e
20	1	0	2+	4420.9±30.8 ^{e,i}	4386.3	-34.6
22	1	0	0+	4931.6±20.2 ^{e,j}	4901.2	-30.4	4897.0	-34.6
24	1	0	4+	5148.7±7.7 ^{e,k}	5144.9	-3.8
26	1	0	0+	5623.2±11.6 ^e	5592.8	-30.4	5632.1	8.9
19	¾	+¾	¾+	3528.3±35.9 ^{l,m}	3524.6	-3.7	3501.8	-26.5
21	¾	+¾	¾+	3954.4±9.2 ⁿ	3964.7	10.3	3944.9	-9.5
23	¾	+¾	¾+	4302.7±21.3 ^{l,o}	4268.8	-33.9	4268.4	-34.3
25	¾	+¾	¾+	4743.4±15.8 ^p	4707.1	-36.3	4698.2	-45.2
19	¾	+½	¾+	3980.4±43.0 ^{l,m}	3997.3	16.9	3989.0	8.6
21	¾	+½	¾+	4440.4±9.2 ⁿ	4439.6	-0.8	4428.1	-12.4
23	¾	+½	¾+	4726.0±32.7 ^{l,o}	4739.3	13.3	4747.7	21.7
25	¾	+½	¾+	5161.4±15.3 ^p	5166.7	5.3	5173.6	12.2
20	2	+2	0+	3484.4±33.9 ^{a,l}	3516.0	31.6	3481.7	-2.7
24	2	+2	0+	4292.4±29.7 ^{a,l,q}	4259.9	-33.1	4245.5	-46.9
20	2	+1	0+	3971.4±33.0 ^{a,l,r}	3986.4	15.0	3966.8	-4.6
24	2	+1	0+	4724.4±28.4 ^s	4721.0	-3.4	4722.8	-1.6
20	1	+1	2+	8448.7±31.9 ^{t,e}	8418.8	-29.9
24	1	+1	4+	9932.2±9.0 ^{t,e}	9923.0	-9.2

^a C. C. Maples, G. W. Goth, and J. Cerny, Nucl. Data **A2**, 429 (1966).

^b These states are not ground states but the lowest excited ½+ states.

^c P. M. Endt and C. Van der Leun, Nucl. Phys. **A105**, 1 (1967).

^d F. Ajzenberg-Selove and T. Lauritzen, Nucl. Phys. **11**, 1 (1959); J. W. Olness, A. R. Poletti, and E. K. Warburton, Phys. Rev. **161**, 1131 (1967).

^e These values were not used in the χ² fit.

^f T. Lauritzen and F. Ajzenberg-Selove, in *Nuclear Data Sheets*, edited by K. Way *et al.* (U. S. Government Printing Office, Washington, D. C., 1962).

^g C. Van der Leun (private communication, 1968) giving the mass excesses of ²⁶Al and ²⁶Mg as -8.9145±0.0021 MeV and -13.1947±0.0018 MeV, respectively.

^h A. E. Blaugrund, D. H. Youngblood, G. C. Morrison, and R. E. Segel (to be published); E. K. Warburton, J. W. Olness, and A. R. Poletti, Phys. Rev. **155**, 1164 (1967).

ⁱ R. D. MacFarlane and A. Siivola, Nucl. Phys. **59**, 168 (1964); J. D. Pearson and R. H. Spear, *ibid.* **54**, 434 (1964).

^j A. Gallman, G. Frick, E. K. Warburton, D. E. Alberger, and S. Hecht, Phys. Rev. **163**, 1190 (1967).

^k A. J. Armini, J. W. Sunier, and J. R. Richardson, Phys. Rev. **165**, 1194 (1967).

^l This work.

^m J. L. Wiza and R. Middleton, Phys. Rev. **143**, 676 (1965); F. A. El Bedewi, M. A. Fawzi, and N. S. Rigk, in *Proceedings of the International Conference on Nuclear Physics, Paris, 1964* (Editions du Centre National

de la Recherche Scientifique, Paris, 1965); R. Moreh and A. A. Jaffe, Proc. Phys. Soc. (London) **84**, 330 (1964).

ⁿ H. Brunnader, J. C. Hardy, and J. Cerny (to be published); D. C. Hensley, Phys. Letters **27B**, 644 (1968); A. B. McDonald, and E. G. Adelberger, *ibid.* **26B**, 380 (1968).

^o S. Mubarakmand and B. E. F. Macefield, Nucl. Phys. **A98**, 97 (1967); B. E. F. Macefield (private communication); J. Dubois, Nucl. Phys. **A104**, 657 (1967).

^p J. C. Hardy and D. J. Skyrme, in *Isotopic Spin in Nuclear Physics*, edited by J. D. Fox and D. Robson (Academic Press Inc., New York, 1966), p. 701; D. Denhard and J. L. Yntema, Phys. Rev. **160**, 964 (1967); G. C. Morrison, D. H. Youngblood, R. C. Bearse, and R. E. Segel, J. Phys. Soc. Japan Suppl. **24**, 143 (1968). These values have been appropriately corrected for the changes noted in footnote e.

^q F. G. Kingston, R. J. Griffiths, A. R. Johnston, W. R. Gibson, and E. A. McClatchie, Phys. Letters **22**, 458 (1966).

^r E. Adelberger and A. B. McDonald, Phys. Letters **24B**, 270 (1967); H. M. Kuan, D. W. Heikkinen, K. A. Snover, F. Riess, and S. S. Hanna, *ibid.* **25B**, 217 (1967); R. Block, R. E. Pixley, and P. Truöl, *ibid.* **25B**, 215 (1967).

^s E. Adelberger and A. B. McDonald, Phys. Letters **24B**, 270 (1967); F. Riess, W. J. O'Connell, D. W. Heikkinen, H. M. Kuan, and S. S. Hanna, Phys. Rev. Letters **19**, 367 (1967).

^t These values are double-Coulomb displacement energies.

shell, including those derived from the data in Table I, is given in the fifth column of Table VI. The numbers quoted are weighed averages of data from the references given, and are intended to be complete up to September, 1968. The table includes only those states for which, in the simplest model, all active nucleons can be considered to be in the $1d_{5/2}$ shell. In addition, for each value of A and T , only multiplets built on ground states are considered, except for those $T=\frac{1}{2}$ odd- A nuclei, whose ground-state spins are not $\frac{5}{2}+$; in these cases the lowest excited $\frac{5}{2}+$ states were used. The $T=\frac{3}{2}$ multiplet with $A=19$ is the only one for which the $\frac{5}{2}+$ states are not known in all nuclei, and consequently the $\frac{3}{2}+$ states were used. In all subsequent fitting, these two $T=\frac{3}{2}$ mass-19 displacement energies were both included and removed; at no time was the over-all fit changed in any way by their inclusion. The last two items in the table are double Coulomb displacement energies which are symbolized, in an obvious notation, by $\Delta E_c(A, T, T_z-2 | T_z)$; their purpose will become apparent.

In Eq. (9) for both the seniority and supermultiplet schemes, the Coulomb displacement energy was given in terms of five parameters a , b , $c^{(1)}$, $c^{(2)}$, and λ . These equations have been fitted to the results in Table VI by treating all five parameters as free, and then minimizing the function χ^2 , where χ^2 is defined by

$$\chi^2 = \sum_{i=1}^M \left(\frac{\Delta E_c(\text{calc})_i - \Delta E_c(\text{expt})_i}{\sigma(\text{expt})_i} \right)^2, \quad (10)$$

M is the total number of experimental values used in the fit and $\sigma(\text{expt})$ is their experimental error. If the averaged experimental errors, as quoted in Table VI, represent a good approximation to the true standard deviation, then the χ^2 test can be applied to the final χ_{\min}^2 obtained by minimizing Eq. (10). If all single displacement energies in Table VI are used, $M=28$, and the number of degrees of freedom of the assumed χ^2 distribution is $(28-5-1)=22$. Under these conditions, for an acceptable fit, χ_{\min}^2 should lie between 11 and 37. Because the method of determining experimental errors on energy measurements is at best inconsistent between different authors, and at worst totally arbitrary, it seems unlikely that such errors are any more than merely indicative of the true standard deviations. Consequently the χ^2 test should in this case be interpreted somewhat loosely.

The variation of χ^2 as a function of λ is shown in Fig. 9 for three cases in both the seniority and supermultiplet schemes. Each point on the graph corresponds to the result of minimizing χ^2 as a function of a , b , $c^{(1)}$, and $c^{(2)}$ for a particular choice of λ . The three cases considered are:

I. For the seniority scheme all the single displacement energies listed in Table VI were used. For the supermultiplet scheme all single-displacement energies were used with the exception of the $T=1$ multiplets for $A=20$ and 24 . As indicated by the fourth line of Table V,

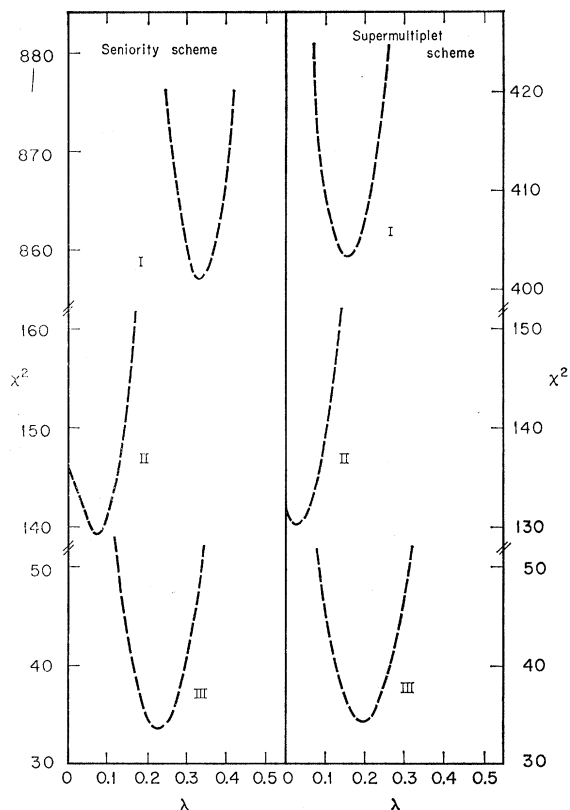


FIG. 9. Plot of the goodness-of-fit parameter (χ^2) versus the strength of A dependence (λ) used in predicting Coulomb-energy differences based on seniority and supermultiplet energy equations. The significance of the curves I, II, and III is discussed in Sec. V of the text.

such multiplets can have either $S=0$ or 1 , and the calculated displacement energies depend upon this choice. However, it is easy to show that when $T_z=+1$, the double-Coulomb displacement energy is independent of S , and consequently the four single-displacement energies involved were replaced by the two double values appearing at the end of the table.

II. The same values were used as in case I except the two energies for ($T=1$, $A=18$) were removed.

III. The same values were used as in case II except the single energy for ($T=\frac{1}{2}$, $A=19$) was also removed.

It is evident from the figure that both case I and case II result in totally unacceptable fits, as evidenced by the values of χ_{\min}^2 . For case III, the seniority and supermultiplet calculations involve, respectively, 19 and 17 degrees of freedom for which the strict range of acceptable χ_{\min}^2 is 8 to 34 and 7 to 31. Considering the reservations stated previously, case III must be deemed an acceptable fit. The values of the parameters λ , a , b , $c^{(1)}$, and $c^{(2)}$ for the minimum χ^2 for both calculations are shown in Table VII in the columns headed "experimental", and the displacement energies calculated using these parameters are listed in columns 6 and 8 of Table VI. It can be seen that there is excellent agreement between the calculated displacement energies and

TABLE VII. Experimental and calculated parameters for the $1d_{5/2}$ shell. The experimental values result from a least-squares fit of the Coulomb displacement energies. The calculated values were obtained using a harmonic-oscillator potential.

Quantity	Seniority scheme		Supermultiplet scheme	
	Experimental ^a	Calculated ^a	Experimental ^a	Calculated ^a
λ	0.23 ± 0.03		0.19 ± 0.03	
a	3673 ± 3		3643 ± 3	
b	209 ± 3	196	211 ± 3	206
$c^{(1)}$	8.14 ± 0.09	4.80	14.40 ± 0.12	
$c^{(2)}$	6.41 ± 0.03	5.28	17.44 ± 0.15	
c	5.89 ± 1.50	4.08	12.89 ± 3.20	3.33
V_0	$(195/184) \pm 14^b$	$168[211]^c$		
V_2		$142[165]^c$		
V_4		$132[140]^c$		
\bar{V}_2	$(148/140) \pm 3^b$	$136[149]^c$		

^a All values, except λ , in keV.

^b The two values shown refer to the beginning and the end of the shell, respectively.

^c The value shown in square brackets was calculated by considering additional correlations between proton pairs; see text.

also between the calculated and the experimental values. Finally, we should remark that the removal of other experimental energies from the fitting procedure does not result in any dramatic changes in either χ_{\min}^2 or the parameter values; in particular, the agreement between the values of λ obtained from both calculations remains good.

The anomalous behavior of the triplet with $A=18$ presents an intriguing analogy with the case of mass 42 (see, for example, Refs. 2 and 3), both multiplets corresponding to $n=2$ in their respective shells $1d_{5/2}$ and $1f_{7/2}$. The behavior of both could be explained as being due to isospin mixing, but it is then unclear why only these multiplets are affected. An alternative hypothesis offered by Nolan *et al.*⁴ to explain the mass-42 data was that the states involved have an anomalously large deformation. Using the values for the parameters a , b , $c^{(1)}$, and $c^{(2)}$ listed in Table VII, we again fitted the mass-18 data by varying λ ; although it was indeed possible to reproduce the ^{18}O - $^{18}\text{F}^*$ energy difference by increasing the interaction radius $\sim 1\%$ from its "average" value, the $^{18}\text{F}^*$ - ^{18}Ne mass difference indicated a *reduction* in the radius by $\sim 1\%$. Such inconsistency makes deformation appear to be an improbable explanation.

The mass-18 and mass-42 triplets were also investigated recently by Bertsch.⁴³ He considered additional correlations between proton pairs generated by excitations into higher shells. These correlations should affect the interaction between the two protons outside the core in the nuclei ^{18}Ne and ^{42}Ti . The experimental evidence, however, seems to indicate that the anomalous behavior of the triplets involves mostly the $T=1$ states in ^{18}F and ^{42}Sc , respectively. In addition, it is not clear why

such correlations should affect only nuclei with $n=2$. As a refinement to the above effect, one may have to consider a change in the interaction with the core. In conclusion, the relationship between the findings of Bertsch and the present analysis is not entirely clear.

Still another possibility for explaining the mass-18 anomaly is suggested by the relatively poor agreement for the $A=19$ doublet. Here, although isospin mixing is unlikely, the wave function is certainly complex as evidenced by the fact that the lowest $\frac{5}{2}^+$ state in ^{19}F is its second excited state. Calculated wave functions⁴⁴ for this state indicate that the $[111]^{22}\text{D}$ component comprises only 50% of the total wave function as compared to an assumed 100% for the supermultiplet scheme; in addition, there are significant $2s$ shell admixtures. Equivalently, in jj coupling, the $(d_{5/2})^3$ component is only 39% of the total strength. Although the similarity of the Coulomb-energy formulas has been used to predict a more general applicability, their accuracy under these conditions is uncertain, particularly considering that there are admixtures from another subshell. Since such admixtures appear to be appreciable only at the beginning of the $1d_{5/2}$ shell, it is possible that they are the cause of our failure to fit the mass-18 and -19 data. However, final verification must certainly await more detailed calculations.

The quantity c cannot be derived directly from the experimental data and the value listed in Table VII was obtained from the experimental quantities $c^{(1)}$ and $c^{(2)}$ by using the theoretical ratio $c/(c^{(1)}+c^{(2)})$. The two-body Coulomb-energy matrix elements V_0 and \bar{V}_2 were obtained in the seniority scheme with the use of Eq. (7). Because of the n dependence of the Coulomb interaction radii defined by Eq. (8), the two-body matrix elements

⁴³ G. F. Bertsch, Phys. Rev. **174**, 1313 (1968).

⁴⁴ J. P. Elliot and B. H. Flowers, Proc. Roy. Soc. (London) **A229**, 536 (1955).

decrease with increasing A . The pairs of values shown for V_0 and \bar{V}_2 refer to the beginning and the end of the $1d_{5/2}$ shell, respectively.

Also shown in Table VII are values for the various coefficients and matrix elements which were calculated⁴⁵ using harmonic-oscillator wave functions. Electromagnetic spin-orbit effects were included³³ in the calculations of $c^{(1)}$ and $c^{(2)}$ in the seniority scheme. There is good agreement between the experimental and calculated coefficients b both in the seniority and supermultiplet scheme. Further, the experimental coefficient a agrees well between the two schemes. The small coefficients c , however, show only qualitative agreement. The experimental values exceed the calculated ones by factors of about 1.4 in the seniority scheme, and about 3.9 in the supermultiplet scheme. This result

TABLE VIII. Mass predictions for neutron-deficient nuclei within the $d_{5/2}$ shell.

Nucleus	Mass excess calculated using:		Garvey-Kelson prediction ^b (MeV)
	Seniority scheme (MeV \pm keV) ^a	Supermultiplet scheme (MeV \pm keV) ^a	
¹⁹ Na	12.965 \pm 25 ^c	12.968 \pm 25 ^c	12.87
²⁰ Mg	17.509 \pm 2	17.510 \pm 2	17.40
²¹ Mg	10.916 \pm 7	10.910 \pm 7	10.79
²² Al	18.059 \pm 30	...	17.93 ^c
²³ Al	6.743 \pm 25	6.758 \pm 25	6.71
²⁴ Si	10.765 \pm 5	10.813 \pm 5	10.72
²⁵ Si ^d	3.828 \pm 8	3.804 \pm 8	3.77

^a The errors quoted only include the experimental error in the masses upon which the predictions depend; see text.

^b Reference 46.

^c The ground-state mass excess is calculated assuming that the lowest $\frac{3}{2}^+$ state in ¹⁹Na is at 0.095 MeV, as in its mirror ¹⁹O.

^d The decay but not the mass of this nucleus is known.

^e This mass was recalculated using the new mass⁴⁷ for ²²F.

seems to indicate that the Coulomb pairing energy is larger than predicted by the calculations, particularly in the supermultiplet scheme. The latter result is probably due to the approximations introduced into the derivation of the supermultiplet equations. It is concluded that pairing in the ground and low excited states is about four times stronger than for the average of the states belonging to the same supermultiplet.

The quantities $c^{(1)}$ and $c^{(2)}$ do not show the expected behavior and their irregularity is probably the result of the underlying simplifying assumptions for the theoretical equations. In addition to contributions from the electromagnetic spin-orbit interaction and the charge-dependent nuclear interaction, the small experimental quantities $c^{(1)}$ and $c^{(2)}$, when treated as adjustable parameters, have to absorb the approximations introduced into the supermultiplet equations, possible con-

⁴⁵ K. T. Hecht (private communication).

TABLE IX. Predicted excitations of unobserved $T=2$ analog states in $1d_{5/2}$ shell nuclei.

Nucleus	J	Excitation energy of $T=2$ state calculated using:	
		Seniority scheme (MeV \pm keV) ^a	Supermultiplet scheme (MeV \pm keV) ^a
²⁰ Na	0+	6.492 \pm 30	6.486 \pm 30
²² Ne	even	14.011 \pm 30 ^b	
	odd	13.987 \pm 30	
²² Na	even	14.760 \pm 30	
	odd	14.727 \pm 30	
²² Mg	even	13.978 \pm 35	
	odd	13.953 \pm 35	
²⁴ Al	0+	5.954 \pm 9	5.971 \pm 9

^a The errors quoted only include the experimental error in the masses upon which the predictions depend.

^b All mass-22 predictions depend upon the mass excess of ²²F being 2.828 \pm 0.030 MeV (Ref. 47).

tributions from isospin mixing (second-order perturbations), the inadequacies of the assumed configurations and coupling schemes, and the approximate nature of the assumed A dependence of the two-body Coulomb matrix elements.

The experimental two-body Coulomb-energy matrix elements V_0 and \bar{V}_2 which were obtained with the use of

TABLE X. Predicted mass differences between different members of $T=\frac{5}{2}$ and $T=3$ isobaric multiplets in the $1d_{5/2}$ shell.

T	Mass difference between analog states in	Mass difference calculated with:	
		Seniority scheme (MeV)	Supermultiplet scheme (MeV)
$\frac{5}{2}$	²¹ Al- ²¹ Mg*	4.492	4.508
$\frac{5}{2}$	²¹ Mg*- ²¹ Na*	4.047	4.054
$\frac{5}{2}$	²¹ Na*- ²¹ Ne*	3.602	3.600
$\frac{5}{2}$	²¹ Ne*- ²¹ F*	3.157	3.145
$\frac{5}{2}$	²¹ F*- ²¹ O	2.712	2.691
$\frac{5}{2}$	²³ Si- ²³ Al*	4.893	4.911
$\frac{5}{2}$	²³ Al*- ²³ Mg*	4.452	4.460
$\frac{5}{2}$	²³ Mg*- ²³ Na*	4.012	4.010
$\frac{5}{2}$	²³ Na*- ²³ Ne*	3.571	3.559
$\frac{5}{2}$	²³ Ne*- ²³ F	3.130	3.108
3	²² Si- ²² Al*	4.915	4.937
3	²² Al*- ²² Mg*	4.472	4.484
3	²² Mg*- ²² Na*	4.029	4.032
3	²² Na*- ²² Ne*	3.586	3.579
3	²² Ne*- ²² F*	3.144	3.127
3	²² F*- ²² O	2.701	2.674

the seniority equations can be compared to two sets of calculated values. One set was calculated⁴⁵ using harmonic-oscillator wave functions as described above. The other set (in square brackets) was also calculated⁴⁴ by using harmonic-oscillator wave functions but additional correlations between proton pairs generated by excitations into higher shells were considered. The experimental values lie in between the two calculated values which seems to indicate that such correlations may be present. However, a similar comparison³ for the $1f_{7/2}$ shell showed no enhancement of the experimental values. It should also be noted that the use of more realistic wave functions such as those which are generated by a reasonable Woods-Saxon well will undoubtedly change the calculated matrix elements to a certain extent.

VI. MASS PREDICTIONS

Using the parameters listed in Table VII it is, of course, possible to calculate any Coulomb displacement energy within the $1d_{5/2}$ shell. Thus, if the mass of any member of a multiplet is known, the masses of all other members can be readily predicted. We have calculated in this manner the masses, as yet unmeasured, of six neutron-deficient nuclei. The results for both schemes are shown in Table VIII,⁴⁶ where the quoted errors only include the experimental error in the masses upon which the predictions depend. For example, the mass of ^{25}Si is derived by adding the displacement energy minus the neutron-hydrogen mass difference (0.7824 MeV) to the mass of the $T=\frac{3}{2}$ analog state in ^{25}Al ; since the experimental error on the energy of that state is ± 8 keV, that is the error quoted in Table VIII. The agreement between calculations with the two coupling schemes is extremely good with the possible exception of ^{24}Si and even for it the discrepancy is only 48 keV. Also shown in the table are the predictions of Kelson and Garvey⁴⁶; they are consistently lower than ours but never by more than 125 keV.

Based on the predictions in Table VIII, the undiscovered nuclei ^{20}Mg and ^{24}Si are certainly stable, since their last proton is bound by more than 2.70 MeV. The nuclei ^{22}Al and ^{23}Al are predicted stable against proton emission by 0.15 and 0.16 MeV, respectively, while ^{19}Na is predicted unstable by 0.36 MeV.

In a similar manner, the excitation energies of $T=2$ states in some $T_z=\pm 1$ and 0 nuclei have been calculated, and the results are tabulated in Table IX.⁴⁷

⁴⁶ I. Kelson and G. T. Garvey, Phys. Letters **23**, 689 (1966).

⁴⁷ R. H. Stokes and P. G. Young, Phys. Rev. **178**, 1789 (1969).

The mass-22 multiplet is assumed to have seniority 2, and consequently the relevant predictions depend upon whether the J of the state is even or odd. Since the ^{22}F ground state is probably $1+$,⁴⁷ the predictions for odd J are more likely correct.

Finally, the mass difference for all remaining members of multiplets within the $1d_{5/2}$ shell have been calculated and are tabulated in Table X. It should be noted that we have tabulated *mass differences*, the neutron-hydrogen mass difference having been included. Thus, for example, if the mass of ^{21}O were known, the mass of its $T=\frac{5}{2}$ analog in ^{21}F could be calculated in the seniority scheme by adding 2.712 MeV.

VII. CONCLUSIONS

A detailed comparison between 28 experimental Coulomb displacement energies in the $1d_{5/2}$ shell and the values obtained with Hecht's Coulomb-energy equations shows very good agreement. Two sets of equations were considered, the one being derived in the low-seniority j - j coupling limit, and the other in the Wigner supermultiplet scheme; the fact that both worked about equally well confirms the expectation that Coulomb energies are relatively insensitive to the assumed coupling scheme. The agreement between the experimental and calculated displacement energies was obtained by treating five coefficients as adjustable parameters and subjecting the data to a least-squares analysis. One of the parameters is related to the Z and N dependence of the charge radius. It was found that the two-body Coulomb-energy matrix elements decrease by about 9% throughout the $1d_{5/2}$ shell. The other parameters make it possible to evaluate experimental matrix elements. Reasonable agreement exists between the experimental and calculated values, where the latter were obtained by using harmonic-oscillator wave functions. However, the experimental Coulomb pairing energy is somewhat greater than the calculated values. Information about the electromagnetic spin-orbit interaction and about the charge-dependent nuclear interaction cannot be extracted at present because of the simplifying assumptions underlying the derivation of the theoretical equations. Despite the assumed simple configurations and coupling schemes the calculated displacement energies reproduced the experimental values very accurately and this fact permitted the masses of certain unknown proton-rich nuclei and excitation energies of unknown isobaric analog states to be predicted with a high probable accuracy.